NUCLEAR SCIENCE AND ENGINEERING: **170**, 66–74 (2012)

Technical Note

Correcting the Cusping Problem in Three-Dimensional Transients Through NEM Modification

Zelmo Rodrigues de Lima*

Instituto de Engenharia Nuclear
Comissão Nacional de Energia Nuclear, Rio de Janeiro, Brazil

and

Aquilino Senra Martinez, Fernando Carvalho da Silva,
and Antonio Carlos Marques Alvim

Programa de Engenharia Nuclear, COPPE
Universidade Federal do Rio de Janeiro, Brazil

Received September 16, 2010
Accepted June 1, 2011

Abstract—*Cross sections are homogenized over an entire node in nodal model implementation. The presence of a control rod (CR) partially inserted in the node has occasioned axial heterogeneity and generates a homogenization problem. If the homogenization process is only the volume-weighted average for nuclear parameters, the calculation of the multiplication factor and power in steady-state problems may mean relevant errors and for time-dependent problems may have caused the well-known cusping problem, which arises in three-dimensional transient simulations with CR motions. The major purpose of this technical note is to introduce an alternative method, based on the nodal expansion method, to deal with partially inserted CRs in nodes. One-dimensional equations, acquired through transverse integration of the neutron diffusion equation, have been modified to formulate the alternative method, which was evaluated in a transient problem. Furthermore, the alternative method gives satisfactory results and corrects the cusping effect in the case analyzed in this technical note.*

I. INTRODUCTION

Because light water reactor spatial heterogeneity in radial planes is more severe than axial heterogeneity, a few nodal method homogenization procedures are restricted to radial planes. However, the presence of control rods (CRs) increases axial heterogeneity, and depending on how this heterogeneity is treated, a cusping problem associated with CRs may arise.

The axial heterogeneities caused by the presence of CRs are problematic for the nodal methods when a CR is partially inserted in the node. A partially rodded node always occurs as soon as the location of the CR tip does not exactly match the interfaces of the axial nodal discretization. The positions of the CRs are varied to compensate for changes in the reactor core, related to fuel depletion, temperature, power level, and reactor shutdown.

Generally, CR motion takes place on a step-by-step basis; each step size is ~1 cm. Therefore, with axial node sizes of 15 to 30 cm, many three-dimensional nodal configurations should include several nodes with partially inserted rods in both steady-state and transient situations.

In nodal model implementation, the cross sections are homogenized over an entire node. The existence of partially inserted CRs in the node causes axial heterogeneity and generates a homogenization problem. If the homogenized cross sections for this node are found using a volume-weighted procedure, the resultant nodal power distribution and the reactor multiplication factor may be

*E-mail: zrlima@ien.gov.br

inaccurate. This problem is accentuated by transients that involve CR motion. A node with a partially inserted CR can lead to a "CR cusping problem," which is named as such because the curve of the power level against the CR position exhibits an unphysical cusp.

This difficulty may be overcome by imposing that the horizontal nodal interface remain localized at each CR tip position. However, depending on the type of calculation and transient, this procedure of node size subdivision may be impractical. As a result, it is more convenient to take into account the ordinary nodalization for all the nodes, rather than subdividing each node, and to consider the partially rodded node as the homogenized one.

Some methods sidestep the cusping problem by using a procedure to find the homogenized parameters in the partially rodded node. For instance, Smith[1] improved the QUANDRY code, which focuses on a quadratic polynomial approximation for neutron axial flux variation inside the node with a partially inserted rod to define equivalent cross sections, weighted in volume and flux. Joo[2] proposed a Collector-Predictor method that also was incorporated into the QUANDRY code. Finally, Gehin[3] employed a scheme that uses node-averaged fluxes in the nodes above and below the partially rodded node to obtain equivalent cross sections, weighted in volume and flux.

This technical note describes an alternative method to treat nodes with partially inserted CRs and that is based on the nodal expansion method[4] (NEM), which was implemented in a spatial kinetic code, to overcome the cusping problem.

II. INTEGRATION OF SPATIAL KINETIC EQUATIONS

The spatial kinetic neutron diffusion equations for two energy groups and six delayed neutron precursor groups are written as follows:

$$\frac{1}{v_g}\frac{\partial}{\partial t}\phi_g(\underline{r},t) = \nabla D_g(\underline{r},t)\nabla\phi_g(\underline{r},t) - \Sigma_{R,g}(\underline{r},t)\phi_g(\underline{r},t) + \sum_{\substack{g'=1\\ g'\neq g}}^{2}\Sigma_{s,gg'}(\underline{r},t)\phi_{g'}(\underline{r},t) + (1-\beta)\chi_g\sum_{g'=1}^{2}\nu\Sigma_{f,g'}(\underline{r},t)\phi_{g'}(\underline{r},t) + \sum_{l=1}^{6}\lambda_l\chi_g C_l(\underline{r},t) \quad (1)$$

and

$$\frac{\partial}{\partial t}C_l(\underline{r},t) = \beta_l\sum_{g'=1}^{2}\nu\Sigma_{f,g'}(\underline{r},t)\phi_{g'}(\underline{r},t) - \lambda_l C_l(\underline{r},t)\ , \quad (2)$$

where

$\phi_g(\underline{r},t)$ = neutron flux in energy group g defined at point $\underline{r}$ and time t

$C_l(\underline{r},t)$ = delayed neutron precursor concentration in precursor group l defined at point $\underline{r}$ and time t.

Equations (1) and (2) are discretized in space and time, as described below.

II.A. Spatial Discretization

The spatial discretization scheme adopted is based on the coarse mesh finite difference (CMFD) formulation.[5] In this formulation, coarse mesh correction factors that modify the classical formulation of finite differences are used according to Eqs. (3) and (4):

$$D_{gxl}^{i,j,k}(t) = \frac{2\left(\frac{1}{a_x^{i-1}}D_g^{i-1,j,k}(t) + \frac{1}{2}f_{gxr}^{i-1,j,k}(t)\right)\left(\frac{1}{a_x^{i}}D_g^{i,j,k}(t) - \frac{1}{2}f_{gxl}^{i,j,k}(t)\right)}{\left(\frac{1}{a_x^{i-1}}D_g^{i-1,j,k}(t) + \frac{1}{2}f_{gxr}^{i-1,j,k}(t)\right) + \left(\frac{1}{a_x^{i}}D_g^{i,j,k}(t) + \frac{1}{2}f_{gxl}^{i,j,k}(t)\right)} \quad (3)$$

and

$$D_{gxr}^{i,j,k}(t) = \frac{2\left(\frac{1}{a_x^{i}}D_g^{i,j,k}(t) - \frac{1}{2}f_{gxr}^{i,j,k}(t)\right)\left(\frac{1}{a_x^{i+1}}D_g^{i+1,j,k}(t) + \frac{1}{2}f_{gxl}^{i+1,j,k}(t)\right)}{\left(\frac{1}{a_x^{i}}D_g^{i,j,k}(t) + \frac{1}{2}f_{gxr}^{i,j,k}(t)\right) + \left(\frac{1}{a_x^{i+1}}D_g^{i+1,j,k}(t) + \frac{1}{2}f_{gxl}^{i+1,j,k}(t)\right)}\ , \quad (4)$$

where

$D_{gxl}^{i,j,k}(t), D_{gxr}^{i,j,k}(t)$ = diffusion coefficients in the left and right faces of a generic node i,j,k in direction x (there are analog equations in directions y and z)

a_x^i = node dimension in direction x

and the correction factors $f_{gxl}^{i,j,k}$ and $f_{gxr}^{i,j,k}$ are given by

$$f_{gxl}^{i,j,k}(t) = \frac{J_{gxl}^{i,j,k}(t) + \frac{2}{a_x^i} D_g^{i,j,k}(t)(\phi_g^{i,j,k}(t) - \psi_{gxl}^{i,j,k}(t))}{\phi_g^{i,j,k}(t) + \psi_{gxl}^{i,j,k}(t)} \tag{5}$$

and

$$f_{gxr}^{i,j,k}(t) = \frac{J_{gxr}^{i,j,k}(t) - \frac{2}{a_x^i} D_g^{i,j,k}(t)(\phi_g^{i,j,k}(t) - \psi_{gxr}^{i,j,k}(t))}{\phi_g^{i,j,k}(t) + \psi_{gxr}^{i,j,k}(t)} \ , \tag{6}$$

where of generic form, $\psi_{gus}^n(t)$ is the average flux in an area transverse to the direction u of node n and $s = l, r$. If the correction factors in Eqs. (3) and (4) are null, we return to the classical methodology of finite differences.

The CMFD formulation uses as input data the diffusion coefficient in the node, $D_g^n(t)$, the average currents and neutron fluxes in the faces of the node are: $J_{gus}^n(t)$ and $\psi_{gus}^n(t)$; and the average flux in the node, $\phi_g^n(t)$, present in Eqs. (5) and (6), are previously obtained by NEM. Equations (1) and (2) can be rewritten in the following matrix form:

$$[v]^{-1} \frac{d}{dt}\underset{\sim}{\Phi}(t) = -[B(t)]\underset{\sim}{\Phi}(t) + (1-\beta)[F(t)]\underset{\sim}{\Phi}(t) + [S(t)]\underset{\sim}{\Phi}(t) + \sum_{l=1}^{6} \lambda_l \underset{\sim}{c}_l(t) \tag{7}$$

and

$$\frac{d}{dt}\underset{\sim}{c}_l(t) = \beta_l[F(t)]\underset{\sim}{\Phi}(t) - \lambda_l \underset{\sim}{c}_l(t) \ , \tag{8}$$

where

$$[B(t)] = \begin{bmatrix} B_1(t) & 0 \\ 0 & B_2(t) \end{bmatrix} ,$$

$$[F(t)] = \begin{bmatrix} F_{11}(t) & F_{12}(t) \\ 0 & 0 \end{bmatrix} ,$$

and

$$[S(t)] = \begin{bmatrix} 0 & 0 \\ S_{21}(t) & 0 \end{bmatrix} , \tag{9}$$

where $[B(t)]$ is a block-heptadiagonal matrix representing the leakage and removal; $[F(t)]$ and $[S(t)]$ are, respectively, the fission and scattering block diagonal matrices; and

$$\underset{\sim}{\Phi}(t) = \begin{bmatrix} \underset{\sim}{\phi}_1(t) \\ \underset{\sim}{\phi}_2(t) \end{bmatrix} ,$$

$$\underset{\sim}{\phi}_g(t) = \begin{bmatrix} \phi_g^1(t) \\ \vdots \\ \phi_g^N(t) \end{bmatrix} , \quad g = 1,2 \ ,$$

$$\underset{\sim}{c}_l(t) = \begin{bmatrix} C_l^1(t) \\ \vdots \\ C_l^N(t) \end{bmatrix} , \quad l = 1,\ldots,6 \ , \tag{10}$$

with N being the total number of nodes. System equations (7) and (8) stand for the semidiscretized form.

II.B. NEM Modification for a Partially Rodded Node

The nodal discretization performed by NEM, or any other nodal method, considers that the nodes are homogeneous, meaning multigroup nuclear parameters that are uniform within each node. However, in some transient problems, we have CR motions; thus, nodes with partially inserted CRs may occur, as shown in Fig. 1. Therefore, it is essential to reformulate the NEM discretization scheme to treat CR motion. NEM is a spatial discretization method using interface currents and is based on the continuity equation and Fick's law. The alternative method described here is the same employed by Martinez et al.,[6] who applied the NEM to the solution of the steady-state problem. In spite of using NEM modified for the nodes with CRs partially inserted for the steady-state case, the main objective of this technical note is to evaluate this version of NEM for the transient problems.

According to Fig. 2, for each of the two regions into which the node was divided (region 1: unrodded node; region 2: rodded node), the multigroup nuclear parameters are uniform and represented by $D_g^{n,type}$ and $\Sigma_{Xg}^{n,type}$ $(X = R, f, s)$, where type = 1 indicates region 1 and type = 2 indicates region 2.

For the problem of a node with a partially inserted CR, the alternative method offers homogenization in volume for D_g and $\Sigma_{gg'}$, as follows:

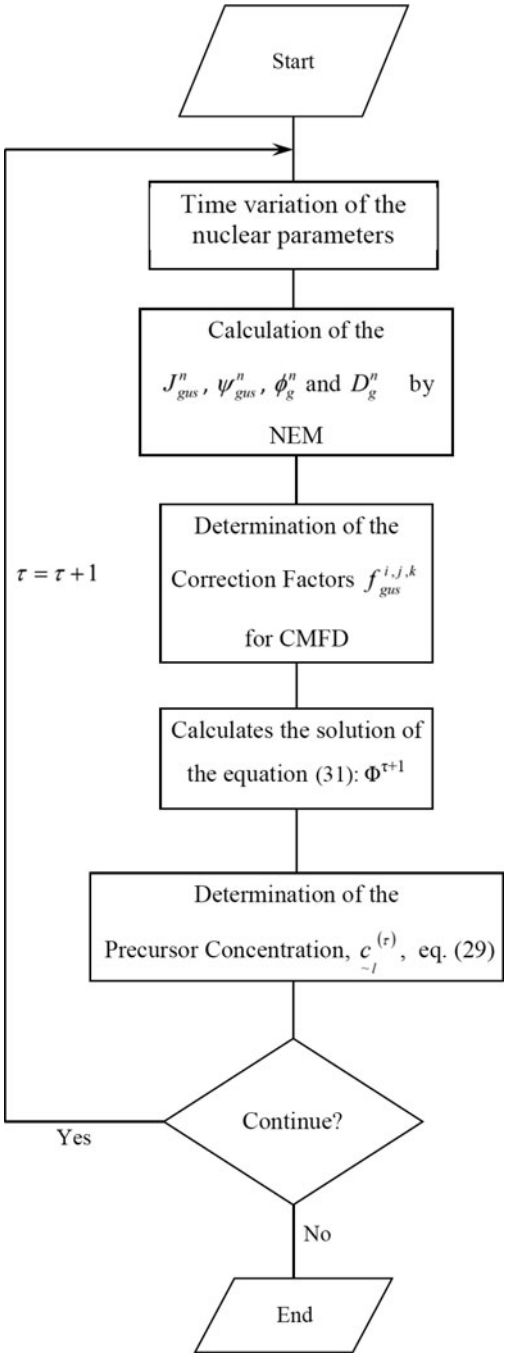

Fig. 1. Sequence of calculation of the proposed method.

$$\hat{D}^n_g = \left(\frac{z^n_c}{a^n_z}\right) D^{n,1}_g + \left(1 - \left(\frac{z^n_c}{a^n_z}\right)\right) D^{n,2}_g \qquad (11)$$

and

$$\hat{\Sigma}^n_{gg'} = \left(\frac{z^n_c}{a^n_z}\right) \Sigma^{n,1}_{gg'} + \left(1 - \left(\frac{z^n_c}{a^n_z}\right)\right) \Sigma^{n,2}_{gg'} \ , \qquad (12)$$

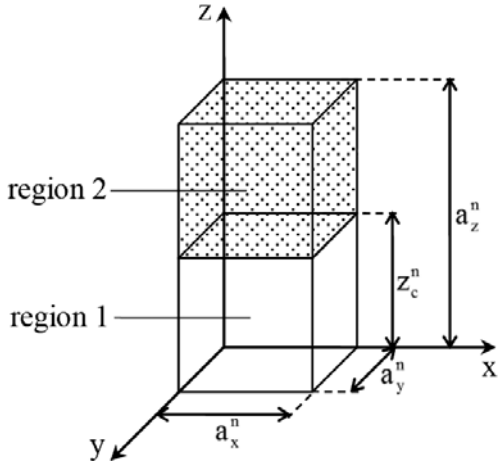

Fig. 2. Diagram of a node n with partially inserted CR.

while the parameters Σ_{ag}, Σ_{fg}, and $\nu\Sigma_{fg}$ are defined as follows:

$$\hat{\Sigma}^n_{Xg} \equiv \frac{1}{V^n \phi^n_g} \int_0^{a^n_x} \int_0^{a^n_y} \int_0^{a^n_z} \times \Sigma_{Xg}(x,y,z)\,\phi_g(x,y,z)\,dxdydz \ , \qquad (13)$$

where

$$\Sigma_{Xg}(x,y,z) = \begin{cases} \Sigma^{n,1}_{Xg} & \text{for } 0 < z < z^n_c \\ \Sigma^{n,2}_{Xg} & \text{for } z^n_c < z < a^n_z \end{cases} \quad \forall (x,y) \ , \qquad (14)$$

and the functional form of $\phi_g(x,y,z)$ is given by

$$\phi_g(x,y,z) = \phi^n_g + \sum_{u=x,y,z} \sum_{m=1}^{2} c^n_{mgu} P_m(u/a^n_u) \ , \qquad (15)$$

where $P_m(u/a^n_u)$ and c^n_{mgu} are, respectively, the same basis functions and the primary coefficients of the following expansion:

$$\psi^n_{gu}(u) = \sum_{m=0}^{4} c^n_{mgu} P_m(u/a^n_u) \ , \qquad (16)$$

commonly used in NEM. The primary coefficients c^n_{0gu}, c^n_{1gu}, and c^n_{2gu} are obtained from a condition of consistency and the diffusion approximation, and high-order coefficients c^n_{3gu} and c^n_{4gu} are obtained from the one-dimensional diffusion equations for functions $\psi^n_{gu}(u)$, by weight residual techniques.

Substituting Eqs. (14) and (15) into (13), we obtain

$$\hat{\Sigma}^n_{Xg} = f^n_{00} \Sigma^{n,1}_{Xg} + (1 - f^n_{00}) \Sigma^{n,2}_{Xg} + (\Sigma^{n,1}_{Xg} - \Sigma^{n,2}_{Xg}) \times \sum_{m=1}^{2} c^n_{mgz} f^n_{0m} / \phi^n_g \ , \qquad (17)$$

where

$$f_{0m}^n \equiv \frac{1}{a_z^n}\int_0^{z_c^n} P_m(z/a_z^n)\,dz$$

$$= \begin{cases} (f_{00}^n)^2 - f_{00}^n & \text{for } m = 1 \\ -2(f_{00}^n)^3 + 3(f_{00}^n)^2 - f_{00}^n & \text{for } m = 2 \end{cases} , \quad (18)$$

with $f_{00}^n \equiv z_c^n/a_z^n$.

The homogenization shown by Eq. (17) modifies the one-dimensional diffusion equations for the functions $\psi_{gu}^n(u)$, employed in the calculation of the secondary coefficients of the expansion defined in Eq. (16). As a result, the equations for the node with a partially inserted CR have the following form:

$$-\hat{D}_g^n \frac{d^2}{d^2u}\psi_{gu}^n(u) + \hat{\Sigma}_{Rg}^n \psi_{gu}^n(u)$$

$$= \chi_g \sum_{g'=1}^{2} \nu\hat{\Sigma}_{fg'}^n \psi_{g'u}^n(u) + \sum_{\substack{g'=1 \\ g'\neq g}}^{2} \hat{\Sigma}_{sgg'}^n \psi_{g'u}^n(u)$$

$$- L_{gu}^n(u) - d_{gu}^n(u) , \quad (19)$$

where

$$d_{gu}^n(u) = (\tilde{\Sigma}_{ag}^n(u) - \hat{\Sigma}_{ag}^n)\psi_{gu}^n(u)$$

$$- \chi_g \sum_{g'=1}^{2} (\nu\tilde{\Sigma}_{fg'}^n(u) - \nu\hat{\Sigma}_{fg'}^n)\psi_{g'u}^n(u) \quad (20)$$

with

$$\tilde{\Sigma}_{Xg}^n(u)\psi_{gu}^n(u) \equiv \frac{1}{a_v^n a_w^n}\int_0^{a_v^n}\int_0^{a_w^n} \times \Sigma_{Xg}(u,v,w)\phi_g(u,v,w)\,dvdw . \quad (21)$$

Substituting Eqs. (14) and (15) into (21), we can conclude the following:

1. For $u = x$ and y,

$$\tilde{\Sigma}_{Xg}^n(u_s^n) = f_{00}^n\Sigma_{Xg}^{n,1} + (1 - f_{00}^n)\Sigma_{Xg}^{n,2} + (\Sigma_{Xg}^{n,1} - \Sigma_{Xg}^{n,2}) \times \sum_{m=1}^{2} c_{mgz}^n f_{0m}^n/\psi_{gus}^n , \quad (22)$$

where

$$\psi_{gus}^n = 2(J_{gus}^{+n} + J_{gus}^{-n})$$

and

$$s = l, r$$

(with $u_l^n = 0$ and $u_r^n = a_u^n$).

2. For $u = z$,

$$\tilde{\Sigma}_{Xg}^n(u_s^n) = \begin{cases} \Sigma_{Xg}^{n,1} & \text{for } s = l \\ \Sigma_{Xg}^{n,2} & \text{for } s = r \end{cases} . \quad (23)$$

It is important to note that according to NEM, $d_{gu}^n(u)$ is considered in the same way as $L_{gu}^n(u)$, that is, through a second-degree polynomial, demonstrated in expansion of the following form:

$$d_{gu}^n(u) = \sum_{m=0}^{2} \beta_{mgu}^n h_m(u/a_u^n) , \quad (24)$$

where

$$\beta_{0gu}^n = 0 , \quad (25)$$

$$\beta_{1gu}^n = \tfrac{1}{2}(d_{gur}^n - d_{gul}^n) , \quad (26)$$

and

$$\beta_{2gu}^n = -\tfrac{1}{2}(d_{gur}^n + d_{gul}^n) , \quad (27)$$

with

$$d_{gus}^n \equiv (\tilde{\Sigma}_{ag}^n(u_s^n) - \Sigma_{ag}^n)\psi_{gus}^n - \chi_g \sum_{g'=1}^{2} (\nu\tilde{\Sigma}_{fg'}^n(u_s^n) - \nu\Sigma_{fg'}^n)\psi_{g'us} . \quad (28)$$

In this sense, we can observe that the multigroup parameters $\hat{D}_g^n$ and $\hat{\Sigma}_{Xg}^n$ found in NEM conventional equations are the parameters $D_g^{n,1}$ and $\Sigma_{Xg}^{n,1}$ for unrodded nodes [with $d_{gu}^n(u) = 0$ in Eq. (19)] and are $D_g^{n,2}$ and $\Sigma_{Xg}^{n,2}$ for nodes with a totally inserted CR [also with $d_{gu}^n(u) = 0$ in Eq. (19)] and are finally given by Eqs. (11), (12), and (13) for nodes with a partially inserted CR [with $d_{gu}^n(u) \neq 0$ in Eq. (19) and given by expansion (24)].

II.C. Time-Dependent Solution

In order to solve the time-dependent equation system, the analytical integration procedure[7] has been adopted for the precursor concentration equation, Eq. (8), whereas the Rosenbrock Generalized Runge-Kutta method with automated time-step-size control[8] has been adopted for the neutron flux in Eq. (7).

In the analytical integration, we have assumed that $\sum_{g=1}^{2} F_{1g}\phi_g(t)$ varies linearly between times t_τ and $t_{\tau+1}$ in Eq. (8), and we integrate analytically in this interval, thus obtaining the expression for $\varsigma^l(t)$ in $t_{\tau+1}$:

$$\varsigma_l^{(\tau+1)} = \varsigma_l^{(\tau)} e^{-\lambda_l \Delta t} + \beta_l \left\{ a_l \sum_{g=1}^{2} F_{1g}\phi_g^{(\tau)} + b_l \sum_{g=1}^{2} F_{1g}\phi_g^{(\tau+1)} \right\} , \quad (29)$$

where coefficients a_l and b_l are defined as

$$a_l = \frac{(1 + \lambda_l \Delta t)(1 - e^{-\lambda_l \Delta t})}{\lambda_l^2 \Delta t} - \frac{1}{\lambda_l}$$

and

$$b_l = \frac{\lambda_l \Delta t - 1 + e^{-\lambda_l \Delta t}}{\lambda_l^2 \Delta t}$$

with

$$\Delta t = t_{\tau+1} - t_\tau \ . \tag{30}$$

The solution to Eq. (7) is given, using the Rosenbrock method, by

$$\underset{\sim}{\Phi}^{\tau+1} = \underset{\sim}{\Phi}^{\tau} + \sum_{s=1}^{4} d_s \underset{\sim}{k}_s^{\tau+1} \ , \tag{31}$$

where the correction vectors $\underset{\sim}{k}_i^{\tau+1}$ are obtained by solving the following system of equations:

$$([I] - \eta \Delta t \underset{\sim}{\boldsymbol{J}}) \underset{\sim}{k}_s^{\tau+1} = \Delta t \underset{\sim}{\boldsymbol{f}} \left(\underset{\sim}{\Phi}(t_0) + \sum_{p=1}^{s-1} \alpha_{sp} \underset{\sim}{k}_p^{\tau+1} \right) + \Delta t \underset{\sim}{\boldsymbol{f}}' \sum_{p=1}^{s-1} \gamma_{sp} \underset{\sim}{k}_p^{\tau+1} \ ,$$

$$s = 1, \ldots, 4 \ , \tag{32}$$

where

$\underset{\sim}{\boldsymbol{J}}, \underset{\sim}{\boldsymbol{f}}$ = Jacobian and the right side of the linear system, respectively

$\eta, d_s, \alpha_{sp}, \gamma_{sp}$ = constants fixed, independent of the problem, where the chosen values are those adopted by Shampine.[9]

The four solutions of Eq. (32), $\underset{\sim}{k}_s^{\tau+1}$, are calculated through a lower-upper matrix decomposition ($[I] - \gamma \Delta t \underset{\sim}{\boldsymbol{f}}'$), followed by four backward substitutions.

During the implementation of the automatic time-step-size control, two solutions of Eq. (31) are used: a third-order solution $\hat{\underset{\sim}{\Phi}}^{\tau+1}$, with different coefficients $\hat{d}_s$, $s = 1, \ldots, 3$, but with the same $\underset{\sim}{k}_s^{\tau+1}$, and a real fourth-order solution $\underset{\sim}{\Phi}^{\tau+1}$. The estimate of the local truncation error is given by

$$\varepsilon = |\underset{\sim}{\Phi}^{\tau+1} - \hat{\underset{\sim}{\Phi}}^{\tau+1}| \ , \tag{33}$$

and the equation applied to automatically adjust the time step size is

$$\Delta t_{next} < 0.9 \Delta t_{prev.} \left(\frac{\varepsilon_0}{\varepsilon} \right)^{1/4} \ , \tag{34}$$

where

Δt_{next} = projected step size for the next step

$\Delta t_{prev.}$ = step in the previous time

0.9 = safety factor

ε = estimated local truncation error

ε_0 = tolerance provided by the user.

TABLE I

Nuclear and Kinetic Multigroup Parameters*

Type	g	D_g (cm)	Σ_{ag} $(\text{cm})^{-1}$	$\nu\Sigma_{fg}$ $(\text{cm})^{-1}$	$\Sigma_{gg'}$ $(\text{cm})^{-1}$	v_g (cm/s)
1	1	1.423913	0.01040206	0.006477691	0.01755555	1.25×10^7
	2	0.356306	0.08766217	0.1127328	0.0	2.5×10^5
2	1	1.425611	0.01099263	0.007503284	0.01717768	1.25×10^7
	2	0.350574	0.09925634	0.1378004	0.0	2.5×10^5
3	1	1.423913	0.01095206	0.006477691	0.01755555	1.25×10^7
	2	0.356306	0.09146217	0.1127328	0.0	2.5×10^5
4	1	1.634227	0.002660573	0.0	0.02759693	1.25×10^7
	2	0.264002	0.04936351	0.0	0.0	2.5×10^5
	Group 1	Group 2	Group 3	Group 4	Group 5	Group 6
β_l	0.000247	0.0013845	0.001222	0.0026455	0.000832	0.000169
λ_l (s^{-1})	0.0127	0.0317	0.115	0.311	1.4	3.87

*Energy release per fission: 3.204×10^{-11} J; $\nu = 2.5$ n/fission.

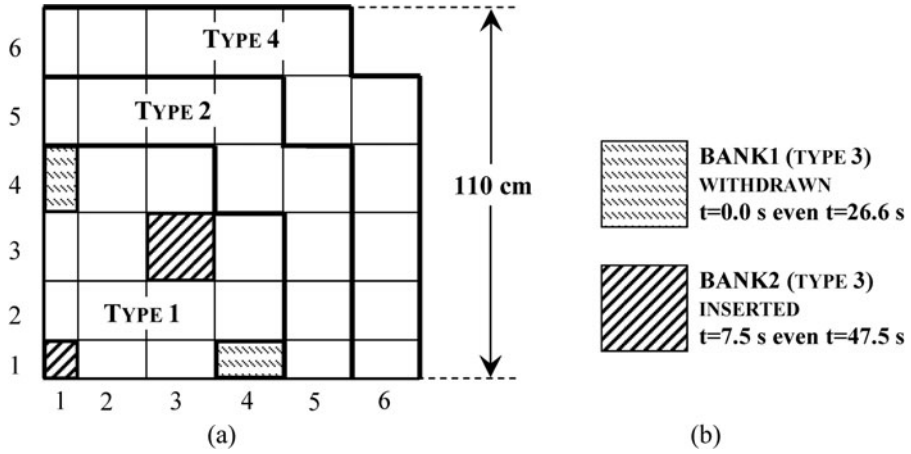

Fig. 3. (a) Radial geometry and (b) movement of CR banks.

Moreover, Δt_{next} is limited by the interval $0.5\Delta t_{prev.} \leq \Delta t_{next} \leq 1.5\Delta t_{prev.}$ to reduce the number of rejected steps and avoid zigzag behavior. The process can be synthesized in the following way. If a time step in the integration is successful, that is, if $\varepsilon < \varepsilon_0$, then the fourth-order solution of Eq. (31) is accepted, and the next time step is chosen according to Eq. (34) and proceeds in time. However, if the time-step-size test fails, that is, if $\varepsilon > \varepsilon_0$, the solution is rejected, and then the previous time step is repeated using a time step size reduced through Eq. (34), until the condition $\varepsilon < \varepsilon_0$ is satisfied.

The alternative method is implemented so that at each step in time, the correction factors given in Eqs. (5) and (6) are updated using NEM, and consequently, the elements of the matrices $[B(t)]$, $[F(t)]$, and $[S(t)]$, inherent to CMFD, are also updated. Figure 2 shows the calculation sequences.

III. RESULTS

In order to verify the alternative method, we adopted as a benchmark the problem introduced by Langenbuch et al.[10] representing a simplified three-dimensional pressurized water reactor model with 77 fuel assemblies. Two energy groups, six delayed neutron precursor groups, and quarter-core symmetry are considered. The core composition and kinetic data are shown in Table I. The

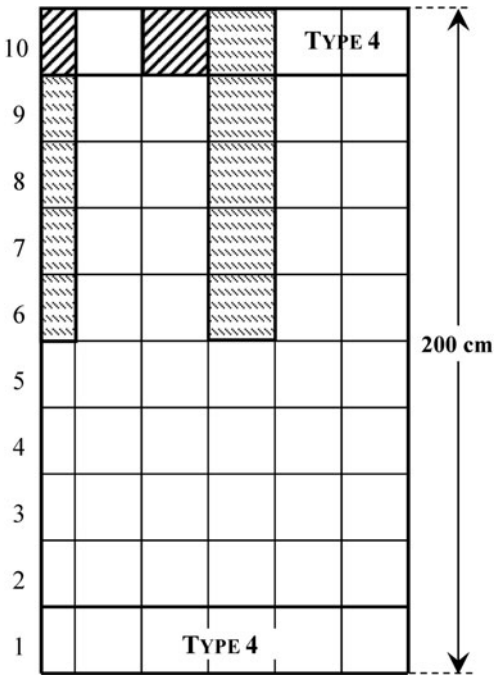

Fig. 4. Axial geometry at the initial instant.

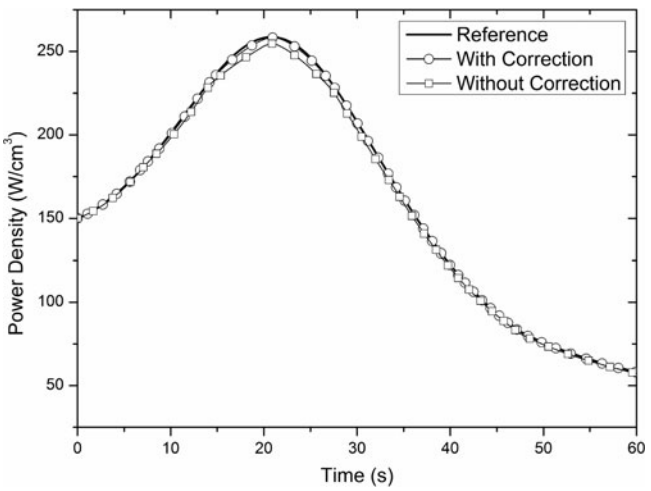

Fig. 5. Variation of power density.

configuration and initial CR positions are illustrated in Figs. 3 and 4, respectively. The alternative method and the method that uses only the volume-weighted average (method without correction) to determine homogenized nuclear parameters in those nodes both used a space mesh of 20-cm width in the three directions and were compared with results obtained for the alternative method, but with a very fine axial mesh of only 2 cm, in a way that the calculation for the fine mesh is considered as the reference.

The transient is initiated by withdrawing bank 1 CRs at a constant speed of 3 cm/s, until completely withdrawn (in 26.7 s). At time $t = 7.5$ s, bank 2 CRs are inserted, at the same speed, for 40 s. The duration of the transient is 60 s.

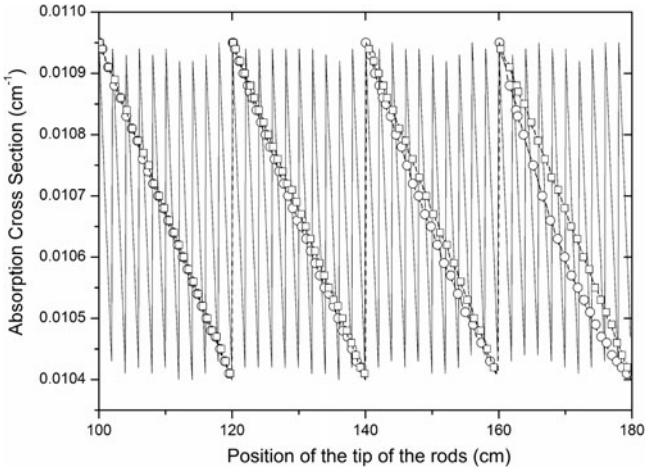

Fig. 6. Variation of the fast absorption cross section as a function of the position of the CR of bank 1.

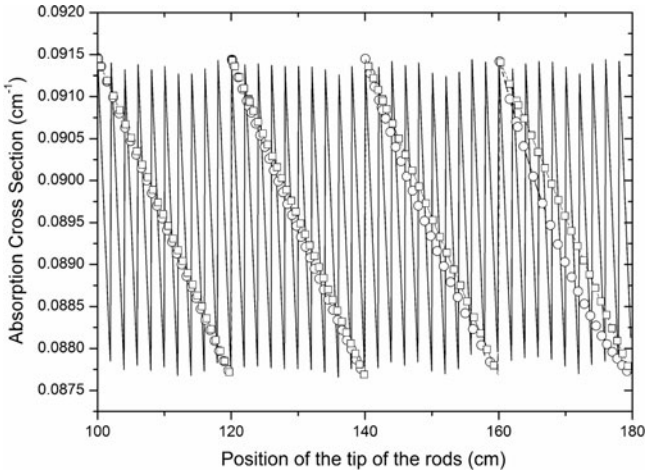

Fig. 7. Variation of the thermal absorption cross section as a function of the position of the CR of bank 1.

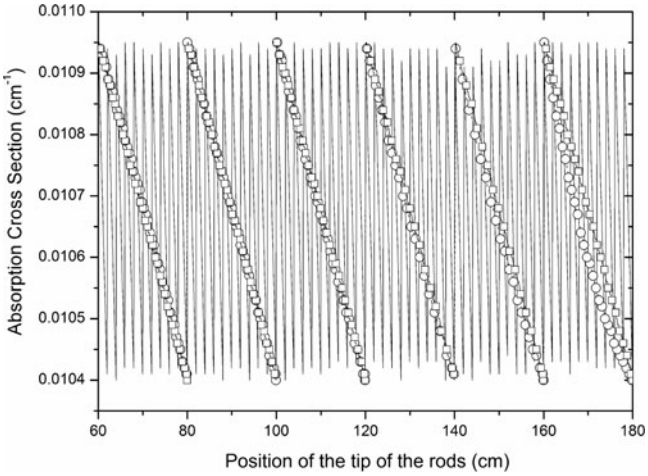

Fig. 8. Variation of the fast absorption cross section as a function of the position of the CR of bank 2.

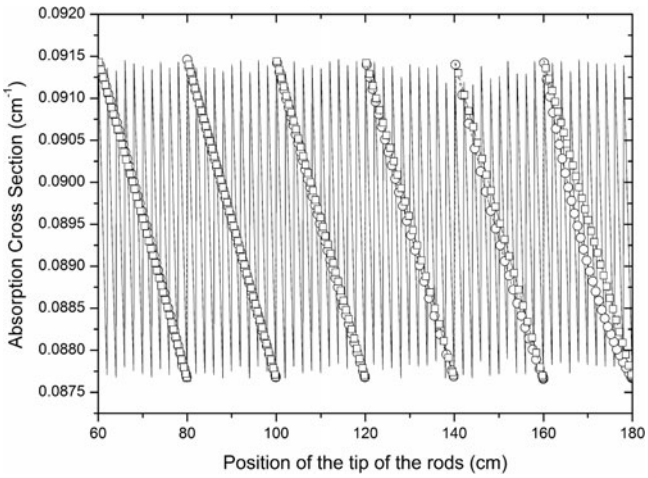

Fig. 9. Variation of the thermal absorption cross section as a function of the position of the CR of bank 2.

Figure 5 shows the plot of nuclear power density against time obtained using the alternative method and the one without correction and the calculations of reference. Figure 5 indicates that the alternative method matches closely the results generated for the fine mesh and corrects the cusping problem.

Figures 6 through 9 are plots of the variations of the absorption cross section as a function of the distance covered by the CR tip.

IV. CONCLUSIONS

This technical note presents an alternative method to treat the heterogeneity caused by a CR partially inserted

in a node. The alternative method is based on NEM with modification of the one-dimensional equation, resulting from the transverse integration of the neutron diffusion equation. This method introduced satisfactory results in the case studied, where the cusping problem was corrected. In a test, the cusping problem caused a small error, $<3\%$ in power density.

For time integration, we employed the Rosenbrock Generalized Runge-Kutta method, which was chosen because it is easy to implement with an automatic time-step-size control. It is obvious that other time integration methods can be used, but it is convenient that they have a truncation error monitoring scheme to control time step size, similar to the alternative method proposed in this technical note.

ACKNOWLEDGMENT

The work was supported by Coordenação de Aperfeiçoamento de Pessoal de Nível Superior (CAPES–Brazil) and Fundação Carlos Chagas Filho de Amparo à Pesquisa do Estado do Rio de Janeiro (FAPERJ–Brazil).

REFERENCES

1. K. S. SMITH, "An Analytic Nodal Method for Solving the Two-Group, Multidimensional, Static and Transient Neutron Diffusion Equation," MS Thesis, Massachusetts Institute of Technology (1979).

2. H. S. JOO, "Resolution of the Control Rod Cusping Problem for Nodal Methods," PhD Thesis, Massachusetts Institute of Technology (1984).

3. J. C. GEHIN, "A Quasi-Static Polynomial Nodal Method for Nuclear Reactor Analysis," PhD Thesis, Massachusetts Institute of Technology (1992).

4. H. FINNEMANN, F. BENNEWITZ, and M. R. WAGNER, "Interface Current Techniques for Multidimensional Reactor Calculations," *Atomkernenergie Kerntechnik*, **30**, 123 (1977).

5. J. M. ARAGONÉS and C. AHNERT, "A Linear Discontinuous Finite Difference Formulation for Synthetic Coarse-Mesh Few-Group Diffusion Calculations," *Nucl. Sci. Eng.*, **94**, 309 (1986).

6. A. S. MARTINEZ, V. PEREIRA, and F. C. SILVA, "A System for the Prediction and Determination of Sub-Critical Multiplication Condition," *Atomkernenergie Kerntechnik*, **64**, 230 (1999).

7. W. M. STACEY, *Space-Time Nuclear Reactor Kinetics*, Academic Press, New York (1969).

8. H. W. PRESS et al., *Numerical Recipes in Fortran*, 2nd ed., Cambrige University Press, New York (1992).

9. L. F. SHAMPINE, "Implementation of Rosenbrock Methods," *ACM Trans. Math. Software*, **8**, 94 (1982).

10. S. LANGENBUCH, W. MAURER, and W. WERNER, "Coarse-Mesh Flux-Expansion Method for the Analysis of Space-Time Effects in Large Light Water Reactor Cores," *Nucl. Sci. Eng.*, **63**, 437 (1977).